Diffusion and thermite reaction process of film-honeycomb Al/NiO nanothermite: Molecular dynamics simulations using ReaxFF reactive force field*

Hua-Dong Zeng(曾华东)[1], Zhi-Yang Zhu(祝志阳)[1], Ji-Dong Zhang(张吉东)[2], and Xin-Lu Cheng(程新路)[1,3,†]

[1] *Institute of Atomic and Molecular Physics, Sichuan University, Chengdu* 610065, *China*

[2] *Key Laboratory of Ecophysics and Department of Physics, School of Science, Shihezi University, Shihezi* 832003, *China*

[3] *Key Laboratory of High Energy Density Physics and Technology of Ministry of Education, Sichuan University, Chengdu* 610064, *China*

(Received 28 December 2016; revised manuscript received 21 February 2017; published online 6 April 2017)

The diffusion and thermite reaction process of Al/NiO nanothermite composed of Al nanofilm and NiO nano honeycomb are investigated by molecular dynamics simulations in combination with the ReaxFF. The diffusion and thermite reaction are characterized by measuring energy release, adiabatic reaction temperature, and activation energy. Based on time evolution of atomic configuration and mean square displacement, the initialization of the thermite reaction process of Al/NiO nanothermite results from the diffusion of Al atoms. Under the microcanonical ensemble, it is found that the adiabatic reaction temperature of the thermite reaction process of Al/NiO nanothermite reaches over 5500 K, and activation energy is 8.43 kJ/mol. The release energy of the thermite reaction process of Al/NiO nanothermite is 2.2 kJ/g, which is in accordance with the available experimental value. With the same initial temperature, the adiabatic reaction temperature of the thermite reaction process of Al/NiO nanothermite has a tendency to decrease dramatically as the equivalence ratio increases. On the basis of chemical bond analysis, the initial temperature and equivalence ratio have great effects on the thermite reaction process, but do not significantly affect the average length of Al–Ni nor Al–O bond. Overall, the thermite reaction of film-honeycomb Al/NiO nanothermite is a complicated process instead of a theoretical equation.

Keywords: molecular dynamics simulations, adiabatic reaction temperature, release energy, mean square displacement

PACS: 61.46.Df, 52.65.Yy, 65.80.–g **DOI:** 10.1088/1674-1056/26/5/056101

1. Introduction

Recently, traditional thermites containing the mixture of aluminum powder and metal oxidizers (MoO_3, Fe_2O_3, NiO, CuO, Bi_2O_3, etc.) in a certain proportion have gradually been replaced by emerging nanothermites that are extensively investigated to serve as nano energetic materials. New fashioned nanothermites have been used for many years such as in fireworks, gunpowder, propellants, airbag materials, welding materials and weapon systems, due to a favorable combination of low cost, environmentally benign reaction products, faster rate of energy release, high energy density, and high reactivity. Over the past few decades, many efforts have been devoted to the further improvement in combustion performance of nanothermites, which was emphatically measured in several aspects including energy release, adiabatic reaction temperature, activation energy, combustion propagation, and so on. The previous experimental results clearly stated that the combustion performance of nanothermite was affected by some main factors: the geometric construction of nanothermites (particle size[1] and equivalence ratio,[2] heating rate[3] and preparation approach.[4] Consequently, a great many novel methods to prepare nanothermites were put forward, such as sol–gel,[5–7] physical mixing with sonication,[8–10] arrested reactive milling,[11] sputtering synthesis,[12,13] and so on. On the other hand, a new series of nanostructured oxidizers (nanowires,[14,15] nanorods,[16] nanotubes,[17] and nano honeycomb[18]) were fabricated and participated in nanothermites as a result of its high specific surface area.

In light of the observed experimental phenomena and results, teams of researchers came up with two distinct mechanisms for fast thermite reaction of the nanocomposites: a melt dispersion mechanism (MDM) and a diffusion oxidizer mechanism (DOM). The MDM[19,20] is suitable for large heating rates (10^6–10^8 K/s), presenting the complete melting of Al core in the fast heating process. Then, the deformation of Al nucleus causes a pressure build-up of 0.1–4.0 GPa, resulting in quiescent shell rupture. At the same time, an unloading pressure wave propagates to the center of the molten Al nucleus. Generation of high tensile pressures cause the molten Al nucleus to disperse into small clusters at high velocity. While DOM[21,22] is suitable for the condition that aluminum is heated at a slow heating rate (10^3 K/s), supposing that the aluminum and oxygen atoms diffuse toward the growing oxide shell to enhance the oxidation rate. Attributed to rapid and violent reaction, however, the microcosmic chemical process of thermite reaction has been rarely explained.

*Project supported by the National Natural Science Foundation of China (Grant Nos. 11374217 and 21363019).

†Corresponding author. E-mail: chengxl@scu.edu.cn

© 2017 Chinese Physical Society and IOP Publishing Ltd

In order to give deep insight into the thermite reaction on an atomic scale, a considerable number of theoretical researches based on molecular dynamics simulations or first principles have been performed. For instance, Henz *et al.*[23] utilized the classical molecular dynamic method to simulate the oxidation process of Al/Al_2O_3 nanoparticles and found that an oxidation ignition mechanism induced an electronic field. Tomar and Zhou[24,25] developed an interatomic potential for each of O, Fe, Al and investigated shock wave propagation of fcc-Al/α-Fe_2O_3 nanocomposites. Furthermore, Shimojo *et al.*[26–28] implemented first-principles molecular dynamics calculation to study the diffusion mechanism at the interface and in electronic process in fast thermite reaction of Al/Fe_2O_3 nanocomposites and developed a concerted metal-oxygen flip mechanism. Those studies argued that conversion of atoms at the interface promoted the thermite reaction. In addition, Farley *et al.*[29] integrated *ab initio* quantum chemical calculations and condensed phase density functional theory to illustrate intermediate I_2O_5 decomposition and surface chemistry between I–O species and Al/Al_2O_3 core/shell particles. Besides, the thermal diffusion and thermite reaction mechanisms of Al-based bimetallic core-shell nanoparticles[30–34] were also studied.

Nickel oxide is a common and easily available oxidizer and has drawn a great deal of attention in the field of nanothermites. For a long time, the thermite reaction of Al/NiO nanocomposites has been one of hotspots in scientific research. Matteazzi and Le Caer[35] primitively studied the solid state reaction of Al/NiO nanocomposites to synthesize Ni/Al_2O_3 nanocomposites. The resulting products were Ni and α-Al_2O_3 after the NiO reduction. Udhayabanu *et al.*[36] investigated the effect of mechanical activation on Al/NiO nanocomposite reaction from high energy ball milling, and demonstrated that amorphous Al_2O_3 existed in the product of NiO reduction and the activation energy for the system is 150 kJ/mol after 20 hours of milling. In order to change the thermal properties of Al/NiO nanocomposite reaction, Bohlouli-Zanjani *et al.*[15] found that the copper additive did not significantly affect the onset temperature of Al/NiO nanothermite comprised of Al nanoparticles and NiO nanowires composites, but caused the energy release to change dramatically. Wen *et al.*[37] first synthesized the NiO nanowires by a hydrothermal method, and exploited sonication to blend the Al nanoparticles, acquiring different Al/NiO nanocomposite mass ratios to measure thermochemical properties of Al nanoparticles and NiO nanowires composites. Through experimental test and thermal analysis, it was found that the different mass ratios have less influence on the onset temperature of Al/NiO nanocomposites. Nevertheless, the release energy of Al/NiO nanocomposites and mass ratio are related by a quadratic function. When the mass of NiO was greater than 35% of the total system, the release energy of Al/NiO nanocomposite was kept at about 1 kJ/g. Moreover, Liu *et al.*[38] studied boron particles that were coated by nano-sized NiO prepared by the precipitation method, in which the combustion performance of B/NiO nanocomposite was improved. The NiO honeycomb nanostructure has been realized by thermal oxidation of a Ni thin film deposited on a silicon substrate.[18,39] The results found that the interfacial contact area of Al/NiO nanothermite had been enhanced by a wide margin. These experimental results indicated that the release energy of the reaction process of Al/NiO nanothermite is increased up to 2.2 kJ/g. Furthermore, it is reported that the adiabatic reaction temperature of Al/NiO nanothermite can reach 3960 K.[40] Gasless thermite reactions were desired for a microinitiator. Among the numerous Al/metal-oxide nanothermites like Al/Fe_2O_3, Al/NiO, Al/CuO, and so forth, Al/NiO nanothermite was reported to produce lower gas. The gas extracted from Al/NiO nanothermite was 10^{-4} mol/g in magnitude, which was approximately 2% of the gas produced from Al/CuO nanothermite and 7.7% from Al/Fe_2O_3 nanothermite.[41] In addition, the Al/NiO nanothermite has a lower onset temperature and releases higher heat output. So Al/NiO nanothermites are considered to be a promising microinitiator.[42] However, to the best of our knowledge, due to a lack of applicable empirical potential, few theoretical researches to systematically shed light on the diffusion and thermite reaction process of film-honeycomb Al/NiO nanothermite are based on molecular dynamics simulations. The NiO nano honeycomb nanostructure might have lots of potential applications due to its porous structure.[43] Therefore, out of these reasons, in this study, we design NiO honeycomb nanostructure as the oxidizer and primarily aim at elaborating the thermite reaction mechanism of film-honeycomb Al/NiO nanothermite. Film-honeycomb nanostructure of Al/NiO nanothermite is specifically selected on the ground that the film-honeycomb Al/NiO nanocomposite has several advantages over previously investigated nanocomposite in some aspects such as lower ignition, enhanced interfacial contact area, reduced impurities and Al oxidation, tailored dimensions, and easier integration into a microsystem to realize functional devices.[18,39] Molecular dynamics simulation in combination with the ReaxFF is performed in this work. In the past decade, the ReaxFF has already been adopted and applied to the various types of reaction system covering combustion[44] and catalyst.[45] It is hoped that the ignition performance of Al/NiO nanothermite would be evaluated on a micro scale. Simultaneously, the effects of equivalence ratio (Φ) and the initial temperature of film-honeycomb Al/NiO nanothermite are studied in detail to enhance the ignition performance of film-honeycomb Al/NiO nanothermite. In addition, thermal properties and diffusion could be systematically investigated and they are characterized by adiabatic reaction temperature,

release energy, activation energy, chemical bond variation in number, and mean square displacement (MSD).

2. Molecular dynamics simulations and models

All the calculations were carried out by the large-scale atomic/molecular massively parallel simulator (LAMMPS) based on the classic molecular dynamics simulations in combination with the ReaxFF for Al, Ni, O developed by Shin *et al.*[46] To accurately describe the formation and cleavage of dynamic bonds in the thermite reaction, the ReaxFF was chosen in this work. The length, width and thickness of NiO nano honeycomb were 5 nm, 5 nm, 2 nm, respectively. The nano honeycomb structure of NiO was comprised of 1536 NiO molecules and had four holes each with a diameter of 0.8 nm as presented in Fig. 1(a). The three different types of film-honeycomb Al/NiO nanothermites, which integrated NiO nano honeycomb with Al nanofilm, were distinguished by their equivalence ratios ($\Phi = 1.20, 1.55, 1.90$). The influence of the space interval on the thermite reaction of nanothermites was reported.[47] The results manifested that the release energy of the thermite reaction of nanothermites became close to the experimental value when the space interval of reactants was 1 nm. Thus, the space intervals between Al nanofilm and NiO nano honeycomb were selected to be 1 nm shown in Fig. 1(b). All simulations were divided into three phases according to the nonperiodic boundary conditions and the time step was set to be 1 fs.

Step 1 Molecular dynamics relaxation. Under the NVT canonical ensemble, the system was kept for 40 ps at 300 K. The potentials of Al/NiO nanothermite tended basically to be steady after 40 ps (see Fig. A1 in Appendix A). It turned out that Al/NiO nanothermite achieved an equilibrium state by molecular dynamic relaxation. As illustrated in Fig. 1(a), the atomic configuration is viewed as the initial nanostructure of Al/NiO nanothermite with Φ of 1.90.

Step 2 Heating process. This simulation procedure was accomplished within the Nose–Hoover thermostat scheme[48] of the NVT canonical ensemble. The Al/NiO nanothermite was heated up to a given temperature (500 K, 600 K and 700 K) with the heating rate of 1 K/ps, separately.

Step 3 Thermite reaction simulation. This step was conducted to simulate an isolated reaction system at 500 K, 600 K, and 700 K in the NVE microcanomical ensemble, separately. Finally, we concretely analyzed the essential features of thermite reaction of Al/NiO nanothermite and compared the characteristics of Al/NiO nanothermite with the available experimental value.

3. Results and discussion

The snapshots of the molecular dynamics simulated nanostructures can be used to investigate the thermite reaction process, especially for studying the diffusions of Al and O atoms in the Al/NiO nanothermite. Figure 1 show the snapshots of Al/NiO nanothermite with Φ of 1.90 and onset temperature of 600 K during the molecular dynamics simulation at different times. After fast heating to 600 K, in consequence of the size effect,[31] the surface of Al nanofilm begins to melt as shown in Fig. 1(b). In order to gain a better understanding of the thermite reaction process, MSDs of Al/NiO nanothermite with Φ of 1.90 in time steps of 400 ps are calculated. Figure 2 exhibits that the MSD of Al atoms is much more than the MSD of NiO nano honeycomb which approaches to zero in a time step ranging from 0 ps to 90 ps. Thereby, we first argue that Al atoms of the Al nanofilm spread toward NiO nano honeycomb before the thermite reaction and the initialization of the thermite reaction is ascribed to the diffusion of Al atoms. Once Al/NiO nanothermite is ignited, Al atoms of the Al nanofilm fleetly migrate into NiO nano honeycomb to form aluminum oxide and leave behind nickel as displayed in Figs. 1(c)–1(d). Meanwhile, the release energy of the thermite reaction of Al/NiO nanothermite makes atoms much more active. MSDs of all atoms quickly increase exponentially after 100 ps in Fig. 2. Subsequently, a reaction area forms between Al and NiO as listed in Fig. 1(d), causing a growing number of Al and O atoms to gradually diffuse into the reaction area. The gradual expanding of the reaction area brings an increase of the reaction temperature by a large margin under the adiabatic condition, and gaseous products set out to vaporize from the reaction area as expressed in Fig. 1(e). After the thermite reaction runs to 200 ps, a great number of nano clusters appear in gaseous condition and sputtering takes place as plotted in Fig. 1(f).

Figure 3 displays the time evolutions of the reaction temperature of film-honeycomb Al/NiO nanothermite for different initial temperatures and Φ values in the molecular dynamic process. After the heating process, the curve of reaction temperature experiences a stable phase, and then increases suddenly in a large range. The results reveal that the turning point of the curve of the reaction temperature represents the beginning of the thermite reaction. Based on the definition in the experimental literature,[49] ignition delay can be regarded as the time interval between the beginning of the heating process and the moment of mutation of the adiabatic reaction temperature. From Fig. 3(a), under the onset temperature of 500 K, Al/NiO nanothermites with Φ values of 1.20, 1.55, and 1.90 have different ignition delay times, which are 336 ps, 483 ps, and 462 ps, respectively. It is also seen in Fig. 3(b) that under the initial temperatures of 500 K, 600 K, and 700 K, the Al/NiO nanothermite with Φ of 1.90 needs 462 ps, 396 ps, and 432 ps to ignite, respectively. In conclusion, these results indicate that the equivalence ratio, the onset temperature, and the ignition delay time are evidently related nonlinearly. Comparing with the experimental data, the ignition delay time is far

less than the experimental value (80 μs),[50] which suggests that the size of the Al/NiO nanothermite, selected in this study is smaller than that of experimental research. Generally, the ignition delay time decreases dramatically on the grounds that the size of the nanothermites decreases from a micro scale to a nano scale.[2]

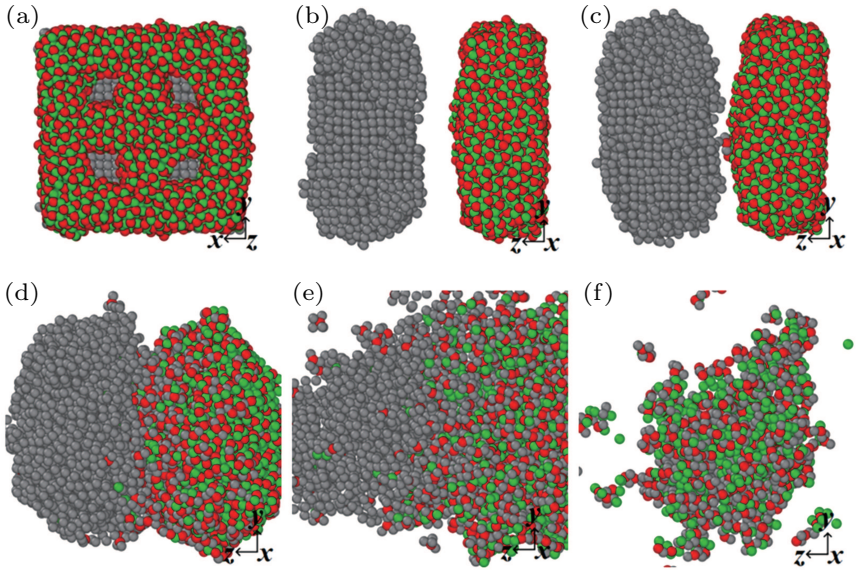


Fig. 1. (color online) Snapshots of atomic configuration. (a) Initial atomic configuration, (b) atomic configuration after the heating process, (c) reaction initiation, (d) reaction 20 ps, (e) reaction 40 ps, (f) reaction 200 ps. The green, red, and gray spheres represent the Ni, O, and Al atoms, respectively.

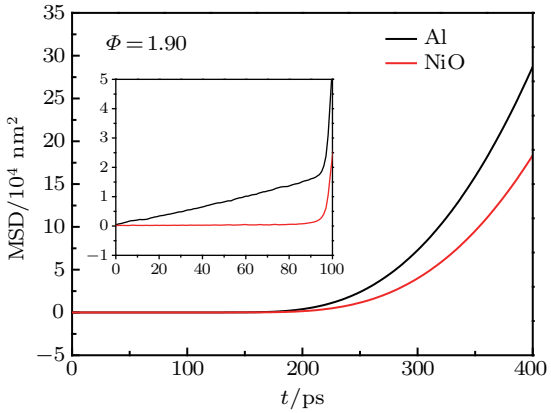


Fig. 2. (color online) Time evolutions of mean square displacement (MSD) of film-honeycomb Al/NiO nanothermite with Φ of 1.90 in time steps of 400 ps.

After the thermite reaction is initiated, a large amount of heat is released. The isolated system is heated rapidly up to about 5000 K as demonstrated in Fig. 3. The adiabatic reaction temperature of the thermite reaction is much larger than available experimental value of 3960 K.[40] See Fig. 3(a), under the same onset temperature of 500 K, the adiabatic reaction temperatures of the thermite reaction for Φ values of 1.20, 1.55, and 1.90 are about 5500 K, 5200 K, and 5300 K, respectively. It is obvious that the adiabatic reaction temperatures of the thermite reaction are different from Φ under the same molecular dynamic condition. In short, the higher the value of Φ, the lower the adiabatic reaction temperature system is. As shown in Fig. 3(b), the adiabatic reaction temperatures of Al/NiO nanothermite with Φ value of 1.90 are 5170 K, 5150 K, and 5200 K for the initial temperatures of 500 K,

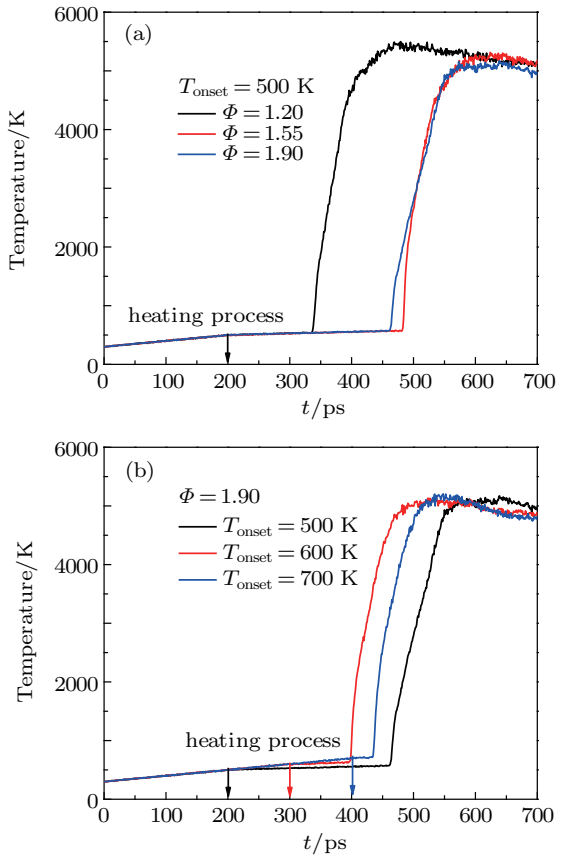


Fig. 3. (color online) Time evolutions of reaction temperature of film-honeycomb Al/NiO nanothermite in time steps of 700 ps, showing (a) temperature profiles with Φ values of 1.20, 1.55, and 1.90 at an onset temperature of 500 K, (b) temperature profiles with Φ values of 1.90 at the onset temperatures of 500 K, 600 K, and 700 K.

600 K, and 700 K, respectively. It unambiguously indicates that the initial temperature has a little influence on release energy from Al/NiO nanothermite under the NVE condition. In a bid to obtain the release energy of the thermite reaction, we simulate the thermite reaction of Al/NiO nanothermite under the initial temperature of 500 K and NVT condition. The variation of total energy of the thermite reaction of Al/NiO nanothermite is plotted in Fig. 4. The total energy of the isolated system tends to be stable when the thermite reaction continues to 400 ps. In other words, the release energy of Al/NiO nanothermite denotes the variation of total energy, which is about 2.2 kJ/g. With the same structure, the release energy is close to the value (2.2 kJ/g)[18] in the experiment, but is far less than theoretical value (3.4 kJ/g). With the same Φ value of 1.23, the heat release value of the reaction reported by Zhang *et al.*[42] is only 0.931 kJ/g.

For the thermite reaction, Al nanofilm and NiO honeycomb nanostructures can be considered as the ingredient of two reactants which need the activation energy E_a to ignite. The value of E_a may be determined by the following equation:[49]

$$D_i = A\exp(E_a/RT). \quad (1)$$

Here, D_i represents the delay time or ignition delay, A the constant value, E_a the energy of activation (ignition), and T the absolute temperature. This equation has been found to be obeyed by a large number of explosives. The curve of $\ln D_i$ versus $1/T$ shown in Fig. 5 clearly indicates that the calculated activation energy of Al/NiO nanothermite with Φ of 1.90 is approximately 8.43 kJ/mol. Due to the size of Al/NiO nanothermite being much less than those of experimental nanoparticles, the calculated activation energy of Al/NiO nanothermite is far less than the experimental value (150 kJ/mol).[36]

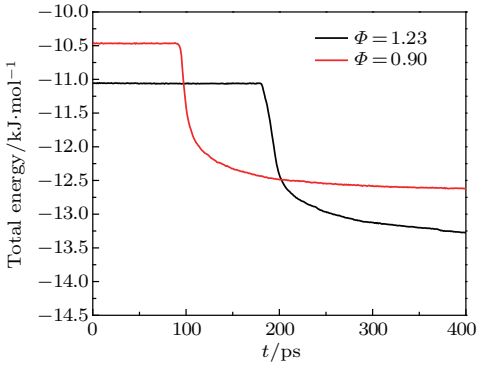


Fig. 4. (color online) Time evolutions of total energy under the onset temperature of 500 K and NVT canonical ensemble.

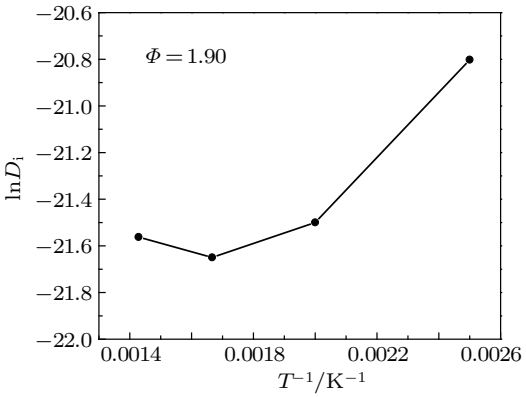


Fig. 5. Curve of $\ln D_i$ versus $1/T$ of film-honeycomb Al/NiO nanothermite with Φ of 1.90.

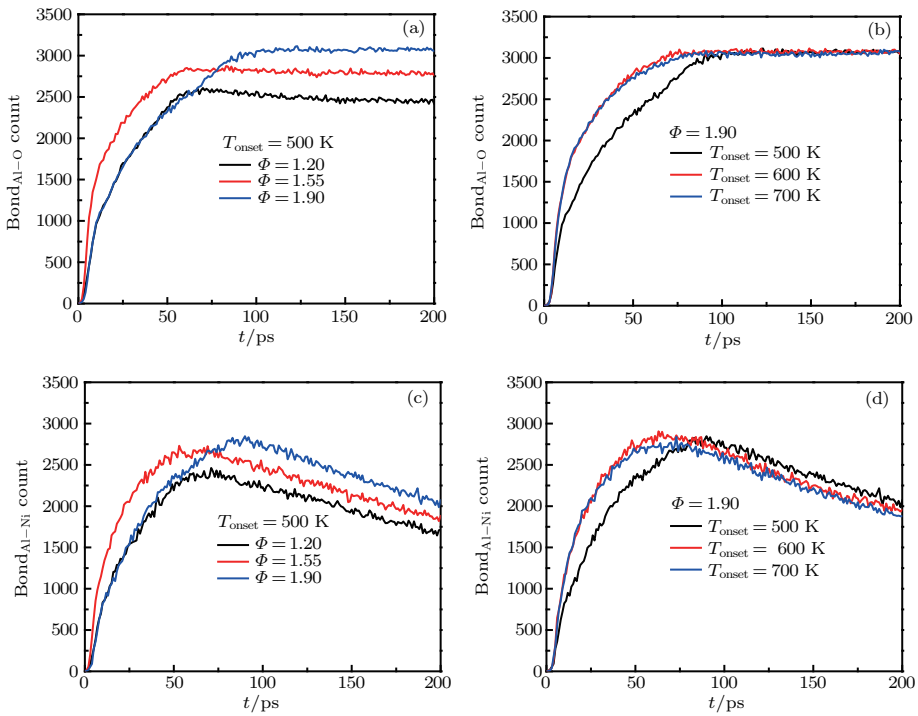


Fig. 6. (color online) Time evolutions of chemical bonds during thermite reaction. (a) Al–O bond profile with Φ values of 1.20, 1.55, and 1.90 under onset temperature of 500 K, (b) Al–O bond profile with Φ of 1.90 for onset temperatures of 500 K, 600 K, and 700 K, (c) Al–Ni bond profiles with Φ values of 1.20, 1.55, and 1.90 under onset temperature of 500 K, (d) Al–Ni bond profiles with Φ of 1.90 for onset temperatures of 500 K, 600 K, and 700 K.

To closely follow the trail of a thermite reaction, changes in the chemical bonds in the thermite reaction process are calculated. Figure 6 exhibits the time evolutions of Al–O and Al–Ni bond at time intervals of 200 ps. It is worth noting that the number of Al–O bonds quickly increases and then tends to be steady after 100 ps as provided in Figs. 6(a) and 6(b). Under the same initial temperature of 500 K, the number of Al–O bonds gradually increases with the increase of Φ in the end of simulation (see Fig. 6(a)). When Φ equals 1.90, the number of Al–O bonds reaches up to 3000 ultimately. Obviously, the number of Al–O bonds is positively correlated with Φ. However, the number of Al–O bonds finally obtained is identical for diverse initial temperatures in Fig. 6(b). It is evidently true that the number of Al–O bonds is barely related to the initial temperature. Unlike the variation of Al–O bonds, the number of Al–Ni bonds is a quadratic function of time as plotted in Figs. 6(c) and 6(d). The peak of Al–Ni bond emerges in a time range from 50 ps to 100 ps. Later, the Al–Ni bond will be more unstable as the reaction temperature rises, leading to the number of Al–Ni bonds falling dramatically. As Fig. 6(c) shows, under the same initial temperature of 500 K, the number of Al–Ni bonds obtained finally increases with Φ. Yet, the number of Al–Ni bonds is negatively correlated with the initial temperature (see Fig. 6(d)). Moreover, the rates of change of the chemical bonds, especially Al–O bonds, are distinctly different at the prophase of thermite reaction. On account of the above, it is not hard to find that the Φ and initial temperature play important roles in the thermite reaction of film-honeycomb Al/NiO nanothermite.

Additionally, in order to analyze the reaction rate, the reaction rate of the thermite reaction is evaluated by calculating the concentration variation of nickel oxide. The concentration of nickel oxide is determined by the following equation:[26]

$$C_{\mathrm{NiO}}(t) = \sum_{i \in O} O_i^{\mathrm{Ni}}(t)/O_i(t). \tag{2}$$

Here, $O_i^{\mathrm{Ni}}(t)$ denotes the number of Ni–O bonds, and $O_i(t)$ the number of all chemical bonds associated with oxygen atoms. Figure 7 clearly shows the time evolutions of $C_{\mathrm{NiO}}(t)$ during the thermite reaction of Al/NiO nanothermite. It is noted that $C_{\mathrm{NiO}}(t)$ decreases rapidly at the beginning of the thermite reaction and tends to be stable in a later stage of the simulation. When the thermite reaction is carried out to 200 ps, $C_{\mathrm{NiO}}(t)$ decreases remarkably from 1.0 to 0.3. Under the same initial temperature of 500 K, the variation of $C_{\mathrm{NiO}}(t)$ gradually enlarges with the augment of Φ, as indicated in Fig. 7(a). Eventually, the remainder of nickel oxide becomes less. When Φ equals 1.90, $C_{\mathrm{NiO}}(t)$ decreases to 0.26, which illustrates the insufficiency of the thermite reaction of Al/NiO nanothermite. Figure 7(b) shows that the rates of change of $C_{\mathrm{NiO}}(t)$ for the initial temperature of 600 K and 700 K are greater than that of $C_{\mathrm{NiO}}(t)$ for the initial temperature of 500 K in the scope from 0 ps to 100 ps. However, the curve of $C_{\mathrm{NiO}}(t)$ under the initial temperature of 600 K almost coincides with that of $C_{\mathrm{NiO}}(t)$ under the initial temperature of 700 K. The variations of $C_{\mathrm{NiO}}(t)$ are entirely equivalent for the initial temperatures of 500 K, 600 K, and 700 K in a late stage of the reaction. It is demonstrated that the reaction rate of Al/NiO nanothermite does not fully depend on the initial temperature. $C_{\mathrm{NiO}}(t)$ does not drop to zero because of the evaporation of unreacted reactants. The simulation results deduce that the thermite reaction process of film-honeycomb Al/NiO nanothermite is inadequate.

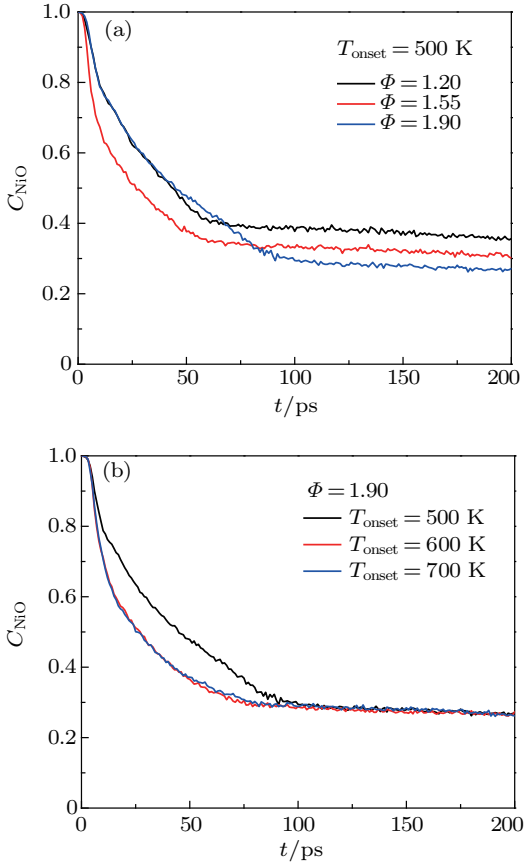


Fig. 7. (color online) Time evolutions of the concentration of NiO during a thermite reaction. (a) NiO concentration profile with Φ values of 1.20, 1.55, and 1.90 under onset temperature of 500 K. (b) NiO concentration profile with Φ value of 1.90 for onset temperatures of 500 K, 600 K, and 700 K.

The distributions of dynamic bonds versus bond length are measured to provide important information about products in the thermite reaction. Figure 8 displays the distributions of Al–O and Al–Ni bonds with respect to bond length after 200 ps of reaction. From Fig. 8(a), it is observed that a large proportion of Al–O bonds are concentrated in the range from 1.4 Å to 1.9 Å, and the number of Al–O bonds increases with increasing Φ value. The average lengths of Al–O bonds are 1.688 Å, 1.692 Å, and 1.690 Å for Φ values of 1.20, 1.55, and 1.90 under the initial temperature of 500 K, respectively. Under different initial temperatures, the distribution of Al–O bond lengths has no apparent difference as indicated in Fig. 8(b). The average length of Al–O bonds is about 1.690 Å, which is not

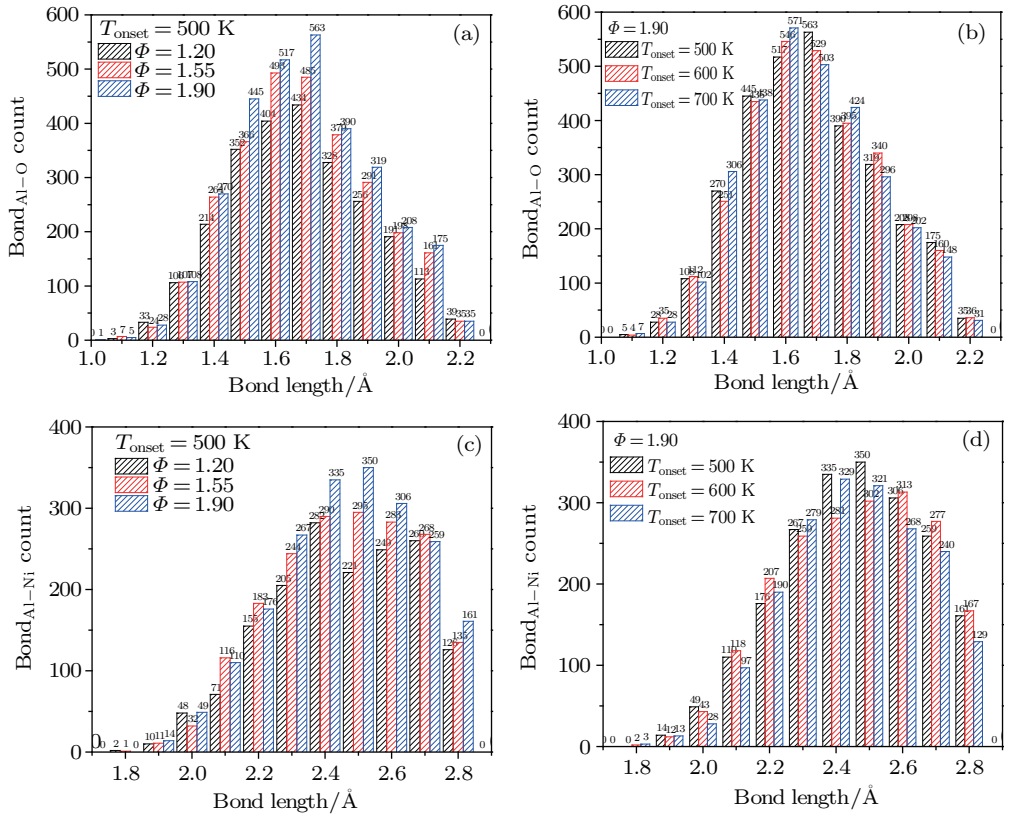


Fig. 8. (color online) The distributions of dynamic bonds with respect to bond length during thermite reaction. (a) Al–Ni bond distributions with Φ values of 1.20, 1.55, and 1.90 under onset temperature of 500 K, (b) Al–Ni bond distributions with Φ of 1.90 for onset temperatures of 500 K, 600 K and 700 K, (c) Al–O bond distributions with Φ values of 1.20, 1.55, and 1.90 under onset temperature of 500 K, (d) Al–O bond distributions with Φ value of 1.90 for onset temperatures of 500 K, 600 K and 700 K.

consistent with that of Al–O bonds in the Al_2O_3 crystal (1.618 Å). It can be assumed that the average length of Al–O bond becomes longer and bond order decreases at high temperature. In Figs. 8(c) and 8(d), the numbers of Al–Ni bonds gathering in a range from 2.4 Å to 2.6 Å are greatly different for different Φ values and initial temperatures. Nevertheless, in molecular dynamics simulations, the average length of Al–Ni bonds has few discrepancies in the range from 2.450 Å to 2.463 Å at different Φ values and initial temperature. Based on the above analysis, the initial temperature and Φ have little effcet on the average lengths of Al–O and Al–Ni bond. Meanwhile, it is verified that the thermite reaction of film-honeycomb Al/NiO nanothermite is not a simply theoretical equation, but a complex chemical process.

4. Conclusions

In the present paper, the three different equivalence ratios of Al/NiO nanothermite ($\Phi = 1.20$, 1.55, and 1.90) with approximately 1 nm in space interval are investigated by using the classic molecular dynamics approach in combination with the ReaxFF. The concentration is taken into account in studying the effects of the equivalence ratio and onset temperature on the thermite reaction and ignition performance under vacuum conditions through calculating the adiabatic reaction temperature, energy release, ignition delay time, and chemical bond variation in the number.

Before the thermite reaction, it is commonly considered that Al atoms spread toward the NiO nano honeycomb and the initialization of thermite reaction results from the diffusion of Al atoms. Once Al/NiO nanothermite is ignited, the thermite reaction will be controlled by the diffusion of Al/NiO nanothermite. Al atoms migrate rapidly into the NiO nano honeycomb to form a reaction area, and much more reactants diffuse into the reaction area so that a sensible increase of the reaction temperature reaches up to 5500 K. In brief, under the same initial temperature, the higher the equivalence ratio of Al/NiO nanothermite, the lower the adiabatic reaction temperature of Al/NiO nanothermite is. However, the initial temperature has very little effect on the adiabatic reaction temperature of Al/NiO nanothermite. The ignition delay time, release energy, and activity energy of the thermite reaction process of Al/NiO nanothermite increase up to 336 ps, 2.2 kJ/g, and 8.43 kJ/mol, respectively. According to chemical bond analysis, the initial temperature and equivalence ratio have a great effect on the thermite reaction process, but do not significantly affect the average length of Al–Ni nor Al–O bond. Above all, the results obtained in this work allow the conclusion that the thermite reaction of Al/NiO nanothermite is a complicated process instead of a theoretical equation. Hence, this study may prove useful for further understanding the thermite reaction process of film-honeycomb Al/NiO nanothermite.

Appendix A: Supporting materials

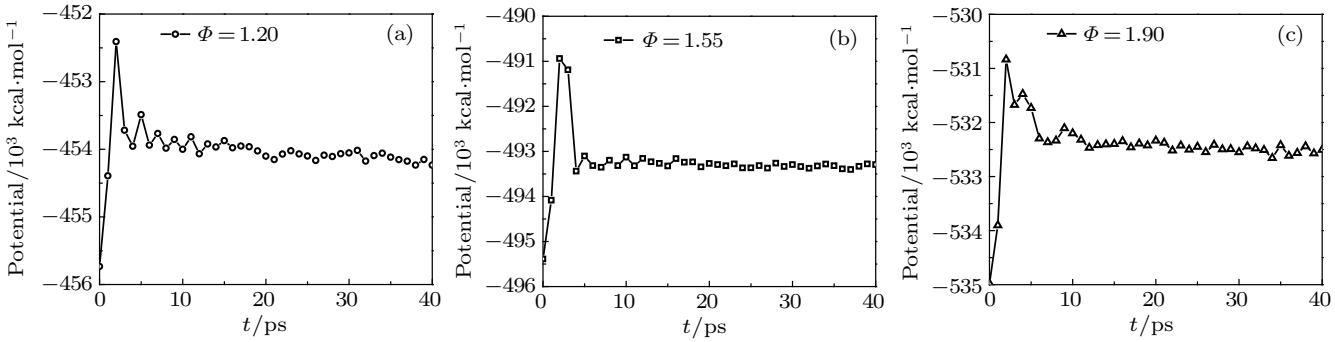


Fig. A1. (color online) Time evolution of potential function during molecular dynamics relaxation. (a) $\Phi = 1.20$, (b) $\Phi = 1.55$, (c) $\Phi = 1.90$.

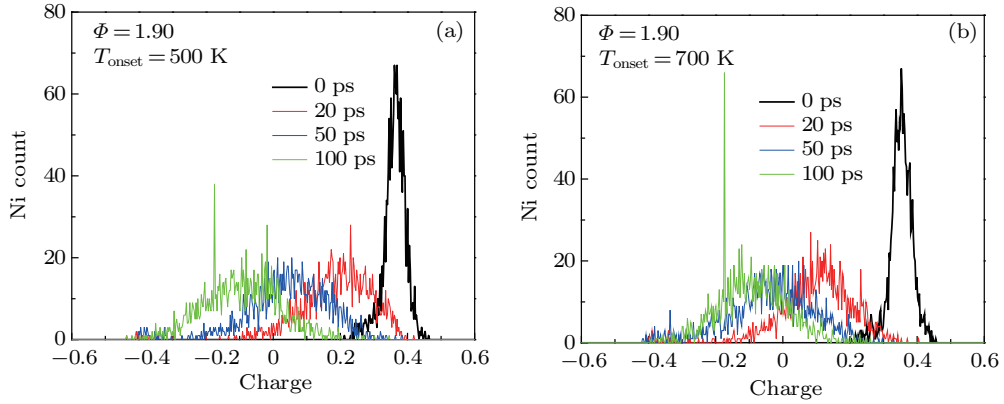


Fig. A2. (color online) The distribution of Ni atom on the charge during thermite reaction. (a) Ni distribution with Φ of 1.90 under onset temperature of 500 K, (b) Ni distribution with Φ of 1.90 for onset temperature of 700 K.

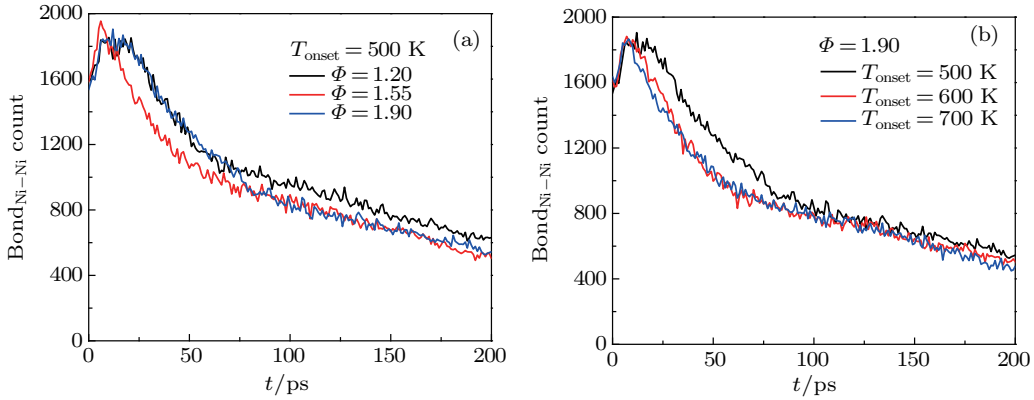


Fig. A3. (color online) Time evolution of chemical bonds during thermite reaction. (a) Ni–Ni bond profile with Φ of 1.20, 1.55, and 1.90 under onset temperature of 500 K, (b) Ni–Ni bond profile with Φ of 1.90 for onset temperature of 500 K, 600 K, and 700 K.

References

[1] Park K, Lee D, Rai A, Mukherjee D and Zachariah M R 2005 *J. Phys. Chem. B* **109** 7290

[2] Granier J J and Pantoya M L 2004 *Combust. Flame* **138** 373

[3] Pantoya M L and Granier J J 2006 *J. Therm. Anal. Cal.* **85** 37

[4] Wang H Y, Jian G Q, Egan G C and Zachariah M R 2014 *Combust. Flame* **161** 2203

[5] Cervantes O G, Kuntz G C, Gash A E and Munir Z A 2011 *Combust. Flame* **158** 117

[6] Shin M S, Kim J K, Kim J W, Moraes C A M, Kim H S and Koo K K 2012 *J. Ind. Eng. Chem.* **18** 1768

[7] Seo H S, Kim J K, Kim J W, Kim H S and Koo K K 2014 *J. Ind. Eng. Chem.* **20** 189

[8] Glavier L, Taton G, Ducéré J M, Baijot V, Pinon S, Calais T, Estève A, Rouhani M D and Rossi C 2015 *Combust. Flame* **162** 1813

[9] Jacob R J, Jian G, Guerieri P M and Zachariah M R 2015 *Combust. Flame* **162** 258

[10] Qiao Z, Shen J, Wang J, Huang B, Yang Z, Yang G and Zhang K 2015 *Compos. Sci. Technol.* **107** 113

[11] Williams R A, Schoenitz M, Ermoline A and Dreizin E L 2014 *Thermochim. Acta* **594** 1

[12] Zhang K, Rossi C, Rodriguez G A A, Tenailleau C and Alphonse P 2007 *Appl. Phys. Lett.* **91** 113117

[13] Bahrami M, Taton G, Conédéra V, Salvagnac L, Tenailleau C, Alphonse P and Rossi C 2014 *Propell. Explos. Pyrot.* **39** 365

[14] Kim D K, Bae J H, Kang M K and Kim H J 2011 *Curr. Appl. Phys.* **11** 1067

[15] Bohlouli-Zanjani G, Wen J Z, Hu A, Persic J, Ringuette S and Zhou Y N 2013 *Thermochim. Acta* **572** 51
[16] Xu D G, Yang Y, Cheng H, Li Y Y and Zhang K L 2012 *Combust. Flame* **159** 2202
[17] Cheng J L, Hng H H, Lee Y W, Du S W and Thadhani N N 2010 *Combust. Flame* **157** 2241
[18] Zhang K L, Rossi C, Alphonse P, Tenailleau C, Cayez S and Chane-Ching J Y 2009 *Appl. Phys. A* **94** 957
[19] Levitas V I, Asay B W, Son S F and Pantoya M 2006 *Appl. Phys. Lett.* **89** 071909
[20] Levitas V I, Pantoya M L and Dikici B 2008 *Appl. Phys. Lett.* **92** 011921
[21] Rai A, Park K, Zhou L and Zachariah M R 2006 *Combust. Theor. Model.* **10** 843
[22] Chowdhury S, Sullivan K, Piekiel N, Zhou L and Zachariah M R 2010 *J. Phys. Chem. C* **114** 9191
[23] Henz B J, Hawa T and Zachariah M R 2010 *J. Appl. Phys.* **107** 024901
[24] Tomar V and Zhou M 2006 *Phys. Rev. B* **73** 174116
[25] Tomar V and Zhou M 2007 *J. Mech. Phys. Solids* **55** 1053
[26] Shimojo F, Nakano A, Kalia R K and Vashishta P 2008 *Phys. Rev. E* **77** 066103
[27] Shimojo F, Kalia R K, Nakano A, Nomura K and Vashishta P 2008 *J. Phys.: Condens Mat.* **20** 294204
[28] Shimojo F, Nakano A, Kalia R K and Vashishta P 2009 *Appl. Phys. Lett.* **95** 043114
[29] Farley C W, Pantoya M L, Losada M and Chaudhuri S 2013 *J. Chem. Phys.* **139** 074701
[30] Levchenko E V, Evteev A V, Riley D P, Belova I V and Murch G E 2010 *Comp. Mater. Sci.* **47** 712
[31] Song P X and Wen D S 2010 *J. Phys. Chem. C* **114** 8688
[32] Nguyen N H, Hu A, Persic J and Wen J Z 2011 *Chem. Phys. Lett.* **503** 112
[33] Wen J Z, Nguyen N H, Rawlins J, Petre C F and Ringuette S 2014 *J. Nanopart. Res.* **16** 2486
[34] Zhang J P, Zhang Y Y, Wang E P, Tang C M, Cheng X L and Zhang Q H 2016 *Chin. Phys. B* **25** 036102
[35] Matteazzi P and Le Caer G 1992 *J. Am. Ceram. Soc.* **75** 2749
[36] Udhayabanu V, Singh N and Murty B S 2010 *J. Alloy. Compd.* **497** 142
[37] Wen J Z, Ringuette S, Bohlouli-Zanjani G, Hu A M, Nguyen N H, Persic J, Petre C F and Zhou Y N 2013 *Nanoscale Res. Lett.* **8** 184
[38] Liu T, Chen X, Xu H X, Han A J, Ye M Q and Pan G P 2015 *Propell. Explos. Pyrot.* **40** 873
[39] Zhang K, Rossi C, Alphonse P and Tenailleau C 2008 *J. Nanosci. Nanotechnol.* **8** 5903
[40] Fischer S H and Grubelich M C 1998 The 24th International Pyrotechnics Seminar, July Monterey CA SAND-98-1176C
[41] Yu C P, Zhang W C, Shen R Q, Xu X, Cheng J, Ye J H, Qin Z C and Chao Y M 2016 *Mater. Desgin* **110** 304
[42] Zhang D and Li X 2015 *J. Phys. Chem. A* **119** 4688
[43] Zhang Q C, Yang X H, Li P, Huang G Y, Feng S S, Shen C, Han B, Zhang X H, Jin F, Xu F and Lu T J 2015 *Prog. Mater. Sci.* **74** 332
[44] Chenoweth K, van Duin A C T and Goddard W A III 2008 *J. Phys. Chem. A* **112** 1040
[45] Chenoweth K, van Duin A C T, Dasgupta S and Goddard W A III 2009 *J. Phys. Chem. A* **113** 1740
[46] Shin Y K, Kwak H, Zou C, Vasenkov A V and van Duin A C T 2012 *J. Phys. Chem. A* **116** 12163
[47] Zhu Z Y, Ma B, Tang C M and Cheng X L 2016 *Phys. Lett. A* **380** 194
[48] Hoover W G 1985 *Phys. Rev. A* **31** 1695
[49] Singh S, Singh G, Kulkarni N, Mathe V L and Bhoraskar S V 2015 *J. Therm. Anal. Calorim.* **119** 309
[50] Valliappan S, Swiatkiewicz J and Puszynski J A 2005 *Pow. Tech.* **156** 164